2022 4th International Conference on Emerging Trends in Electrical, Electronic and Communications Engineering (ELECOM) | 978-1-6654-6697-4/22/$31.00 ©2022 IEEE | DOI: 10.1109/ELECOM54934.2022.9965223

A comparative analysis of Maximum Power Point Tracking (MPPT) Techniques of a Solar Panel

Yogindersing Gajadur
Department of Electrical and Electronic Engineering
University of Mauritius
Réduit, Mauritius
yogindersing.gajadur@gmail.com

S Z Sayed Hassen
Department of Electrical and Electronic Engineering
University of Mauritius
Réduit, Mauritius
sayed.hassen@gmail.com

***Abstract*—A photovoltaic panel operates along a non-linear Power-Voltage (P-V) curve. When a load is directly connected to the photovoltaic (PV) panel, the output voltage of the panel changes with the delivered current. The panel's P-V characteristic shows that the power it delivers is maximum at one particular operating combination of voltage and current, called the Maximum Power point (MPP). However, this MPP is not static and it shifts with varying loads as well as due to changes in temperature, solar irradiance level. This paper compares the performance of three MPPT techniques namely, Perturb and Observe (P&O), Sliding Mode Control (SMC) and Fractional Short-Circuit Current (FSCC) of a given PV system through simulation. The PV system is modeled in MATLAB/Simulink environment and it consists of a 20 W PV module supplying power to a resistive load through a DC-DC Boost converter. Algorithms of the three aforementioned MPPT control techniques (PO, FSCC, and SMC) are developed and simulated under changing solar irradiance level and their performances are compared. It was observed that Sliding Mode Control technique has the fastest tracking time and produced the least oscillations at steady state.**

Keywords—Maximum Power Point Tracking, Fractional Short Circuit Current, Sliding Mode Control, Perturb and Observe.

I. INTRODUCTION

The amount of the sun's power radiated to earth is about 1.8×10^{14} kW [1] and if harvested properly has the potential to completely cut down our dependency on fossil fuels. However, the lack of suitable locations to implement PV farms and the low efficiencies of commercially available PV panels limit our capacity to capture much of this energy [2].

The least efficient a PV system is, the more PV panels would be required to meet a given power demand. Furthermore, more panels would bring with it a cascade of other expenses as inverters and wires of higher ratings would be required. As a consequence, the Life Cycle Cost (LCC) of the system increases and the savings (if any) reduced. It is therefore of utmost importance to operate a PV system at its MPP to maximize efficiency.

PV panels operates along a non-linear P-V curve. That is, as the voltage across the terminal's changes, so will the power in a non-linear way [3]. For a single PV panel with even irradiation, a maximum power peak is observed. There may even be more than one peak when multiple PV panels are connected through bypass diodes under uneven irradiance [4].

If a load is directly connected to the panel, the operating point, which is the intersection between the load characteristic and the Power-Voltage curve of the panel, doesn't necessarily match the MPP. Moreover, for a given load, the MPP varies with temperature and irradiance [3].

In order to ensure that maximum power is obtained from the panel, a DC-DC converter, acting like an impedance matching device, is used as an interface between the PV panel and the load. By varying the control signal, which represents the duty cycle of the converter, we can drive the operating point of the system to reach the MPP [5].

The control signal is generated by a MPPT algorithm on the basis of PV panel's output current and voltage measurement. A significant number of MPPT techniques have been developed over the years. The algorithms are often embedded into optimizers, inverters and charge controllers themselves. In this paper, three MPPT techniques, namely, P&O, SMC and FSCC are investigated and their performance compared. These three were our preferred choice to be able to compare the performance of three very dissimilar algorithms.

II. PHOTOVOLTAIC SYSTEM MODELING

This section is devoted to the modeling of a photovoltaic system using a single-diode model (Fig.1). The model takes both irradiance and temperature as input variables. Parameters for the ACOPOWER HY020-12M solar panel were used to obtain the solar cell parameters, as per derived equations [6]. The single diode solar cell is implemented as a Simulink block model. This system was then used to implement the MPPT algorithm.

A. Design of a model of the Photovoltaic Module

The effects of irradiance and temperature on photocurrent I_{ph}, were modeled by the equation:

$$I_{ph} = I_{ph(STC)} \cdot \frac{G}{G_{STC}} \cdot [1 + \alpha_1 \cdot (T - T_{STC})] \quad (1)$$

And the module's output current was given by:

$$I = I_{ph} - I_{sat} \cdot \left(e^{\frac{V + I.R_s}{\eta V_t}} - 1 \right) - \frac{V + I.R_s}{R_p} \quad (2)$$

The unknown parameters used in (1) and (2) were calculated as follows:

$$V_t = \frac{k.T}{q} \quad (3)$$

$$I_{sat} = C.T^3.e^{-\frac{E_{gap}}{kT}} \quad (4)$$

$$R_s \approx -\frac{dV}{dI}\Big| \; at \; v = v_{oc} \quad (5)$$

$$R_p \approx -\frac{dV}{dI}\Big| \; at \; I = I_{sc} \quad (6)$$

978-1-6654-6697-4/22/$31.00 ©2022 IEEE

where I_{sat} is the diode's saturation current (A), η is the diode's ideality factor, C is the temperature coefficient (V/K), α_1 is the temperature coefficient of I_{sc} (A/K), T is the absolute temperature (K), k is the Boltzmann constant (1.3806503×10−23 J/K), E_{gap} is the band gap of semiconductor material (for crystalline silicon: E_{gap} = 1.124 eV = 1.8×10−19 J), G is the irradiance (W/m^2), I_{ph} is the photocurrent (A), q is the electronic charge (1.60217646×10−19 C), R_s is the series resistance (Ω), R_p is the parallel resistance (Ω), I is the PV module's output current (A), V is the voltage at the terminals (V), V_{oc} is the open circuit voltage (V), I_{sc} is the short-circuit current (A), *STC* is the standard test conditions of 1000 W/m^2 at 298.15 K.

The Single Diode model in Fig.1 was built as per equations (1) and (2) in Simulink.

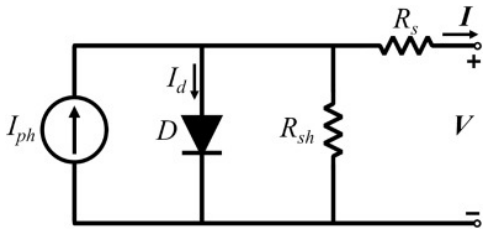

Fig. 1. Single Diode model of a PV module

B. Verification of the simulated PV Model

The system was simulated at different irradiance levels and it was observed that voltage and current measurements obtained were as expected and the simulated parameters were within 2% of the datasheet values. Fig. 2 is the P-V curve obtained from the model at 1 kW/m^2. Table I compares data from datasheet and data obtained in simulation.

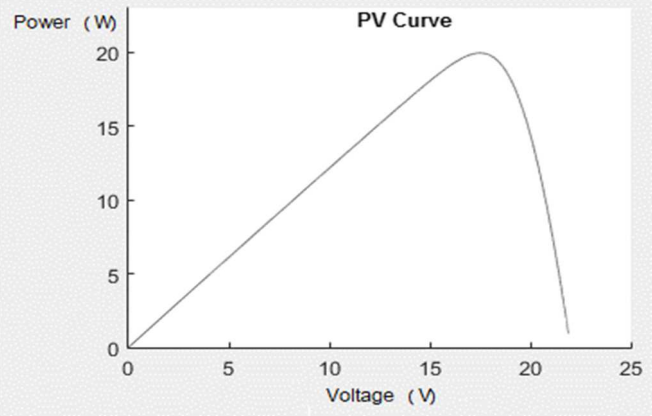

Fig. 2. P-V curve

TABLE I. PARAMETER VERIFICATION FOR THE SIMULATED MODEL

	Simulated values	*Datasheet values*
I_{sc} (A)	1.23	1.23
V_{oc} (V)	21.7	22.0
MPP (W)	19.95	20.0
V_{mpp} (V)	17.66	17.50
I_{mpp} (A)	1.13	1.14

III. MPPT CONTROL PRINCIPLE-IMPEDANCE MATCHING

Maximum power can be delivered to the load when the load line crosses the I-V curve of the PV module at MPP. This cannot happen under varying temperature and irradiance conditions. The characteristic of load and source matching or impedance matching is done with the help of a DC-DC converter and the duty cycle of the converter is decided by the MPPT algorithm. In this simulation, a Boost Converter was chosen because of its higher efficiency [7] and its simple design. A PWM frequency of 31 kHz was used as this frequency can easily be generated by an Arduino Microcontroller in practice. As stated in [8], the minimum value of inductance required to operate in Continuous Conduction Mode (CCM) can be calculated as follows:

$$L = \frac{D(1-D)^2 R_o}{2f_s} \tag{7}$$

Where, L is the inductance (H), D is the duty cycle that yield a maximum L, R_o is the resistive load (Ω). Since the inductor's current is the same current flowing through the PV module, CCM is required. For the set of simulation done here, a 1 mH inductor was chosen. The duty cycle required to operate at MPP is given by:

$$D = 1 - \sqrt{\frac{R_{eq}}{R_o}} \tag{8}$$

$$R_{eq} = \frac{V_{mpp}}{I_{mpp}} \tag{9}$$

Where R_{eq} is the equivalent resistance at MPP (Ω), V_{mpp} is the MPP voltage (V) and I_{mpp} is the MPP current (A). For load matching to occur, R_o should be greater than R_{eq}. Table II contains simulated values of R_{eq} at different irradiances. As can be observed, R_{eq} is always lower that 150Ω, hence 150Ω was used as an appropriate resistive load for this system.

TABLE II. SIMULATED PARAMETERS

Irradiation (kW/ m^2)	*V_{mpp} (V)*	*I_{mpp} (A)*	*$R_{optimum}$ (Ω)*	*P_{mpp} (W)*	*Duty cycle*
0.1	17.02	0.1147	148.4	1.952	0.5391
0.4	17.69	0.4588	38.56	8.117	49.30
0.7	17.71	0.7993	22.16	14.16	61.57
1.0	17.50	1.140	15.35	19.95	68.01
1.3	17.24	1.477	11.67	25.46	72.10

IV. MAXIMUM POWER POINT TRACKING ALGORITHMS

In this section, we provide some insight on the three different MPPT techniques proposed.

A. The Perturb and Observe Algorithm

This technique involves the application of a small perturbation (in duty cycle) to the PV system and then determining the direction of power change. The sign of power change provides the algorithm with information as to the direction to apply the next perturbation so as to arrive at the MPP. The small perturbation is a small change in duty cycle.

A change in duty cycle will indirectly create a small change in the output voltage. Depending on the segment of the P-V curve the operating point is, a change in voltage will either bring a positive or negative power change. The duty cycle is updated in such a way as to make the change in power positive. The algorithm is depicted by the flowchart of Fig. 3.

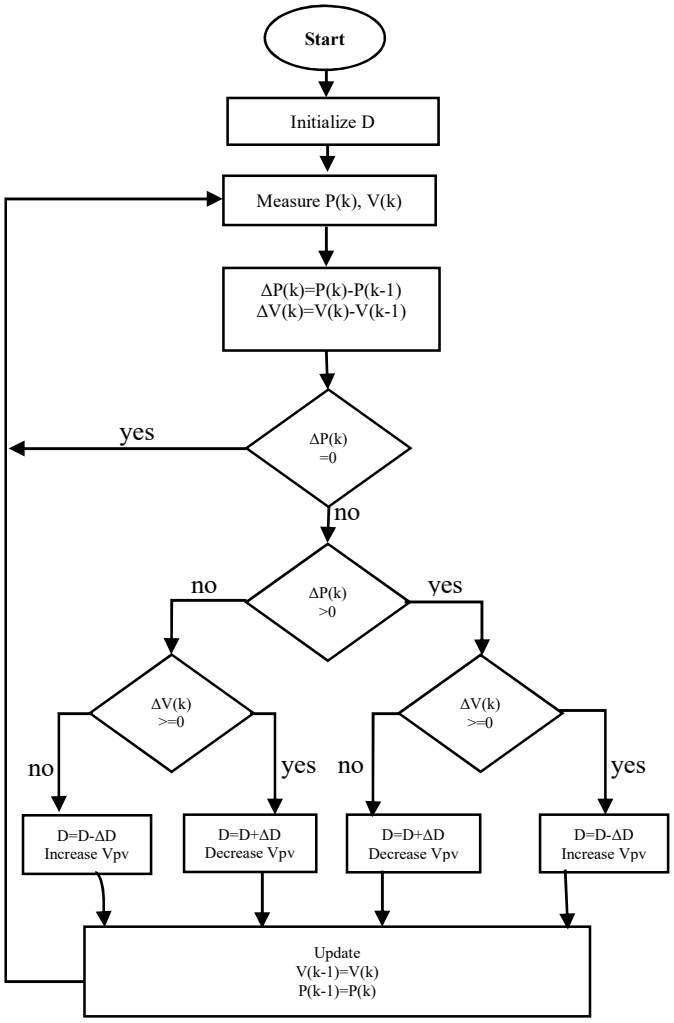

Fig. 3. Flowchart of Perturb and Observe algorithm

B. Fractional Short-Circuit Current Technique

This technique uses the fact that the current at MPP is approximately equal to 0.86 times the I_{sc}. The value of 0.86 is obtained by conducting a lot of experiments on commercially available PV modules, see [6]. By measuring I_{sc} at regular time intervals, I_{empp}, the estimated maximum power point current, can be estimated as:

$$I_{empp} = k_i \times I_{sc} \tag{10}$$

where, k_i is assumed to be a constant. The main disadvantage of such technique is that the MPP will be estimated and the operating point may not be the real MPP. The algorithm is depicted by the flowchart of Fig. 4. Power flow is interrupted at regular intervals when I_{sc} is being measured. If the current is greater or lower than I_{sc}, the duty cycle is updated accordingly to bring the current to the estimated I_{mpp}.

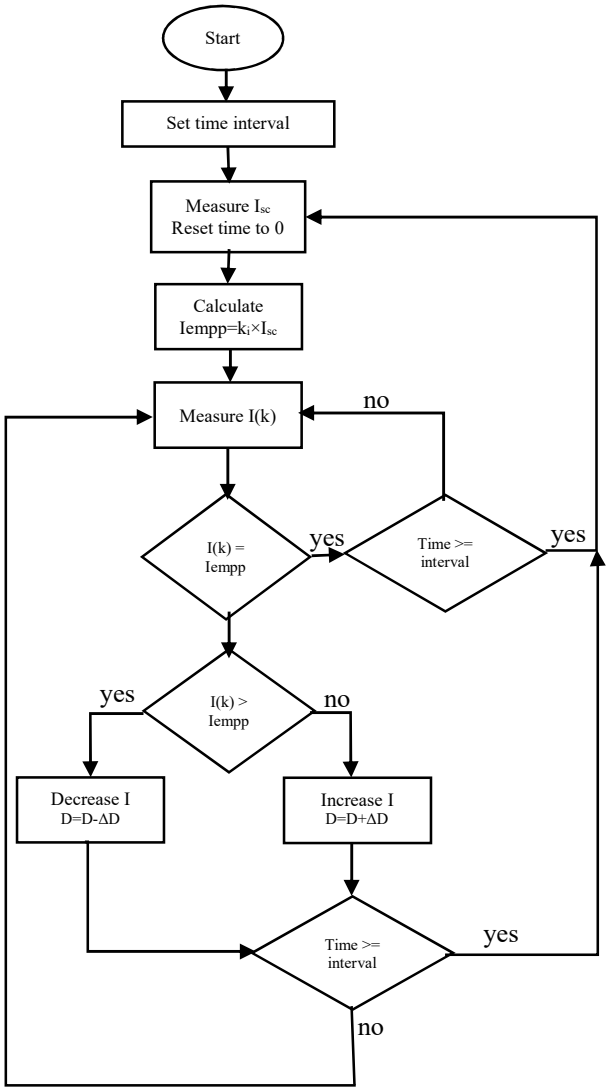

Fig. 4. Flowchart of Fractional Short-Circuit Current technique

C. Sliding Mode Control

This technique involves the derivation of a mathematical surface, S, onto which the gradient of the PV curve is zero. The system is made to slide on this surface. The following set of equations below describes the surface S, where P is the power from the PV panel.

$$\frac{dP}{dV} = 0 \; and \; \frac{dP}{dI} = 0 \tag{11}$$

Using the product rule, equation (11) is simplified to:

$$\frac{dP}{dI} = \frac{d(V \times I)}{dI} = V + I\frac{dV}{dI} = 0 \tag{12}$$

At V= V_{mpp} and I= I_{mpp}, the following equation is true:

$$\frac{dV}{dI} + \frac{V}{I} = 0 \tag{13}$$

Equation (13) can be written in terms of time derivatives as follows:

$$\frac{dV/dt}{dI/dt} + \frac{V}{I} = 0 \tag{14}$$

We define the surface, S, such that on this surface, the output is always a scalar value:

$$S = \frac{dV/dt}{dI/dt} + \frac{V}{I} \quad (15)$$

To operate on S, there should be a discontinuous control signal U, which always attracts the state vectors of the system onto this surface irrespective of where the system started. A sliding action occurs when the path remains on S, when it is started on it, or driven towards S when started outside of it. U can be defined as:

$$U = \frac{1}{2}(1 + Sign(S)) \quad (16)$$

$$U = \begin{cases} 1 & S > 0 \\ 0 & S \leq 0 \end{cases} \quad (17)$$

Where, U=1 and U=0 are two one-dimensional vectors f_1 and f_2 respectively. Assuming the system starts at S>0, f_1 only is used to pull the operating point towards the switching surface S. If it starts at S<0, f_2 only is used to pull the operating point towards S. Once the operating point in on S, there is a high frequency switching between f_1 and f_2 that causes sliding to occur along S. This is illustrated in Fig. 5. U is applied directly to the switch of the boost converter and there is no need to generate a PWM signal.

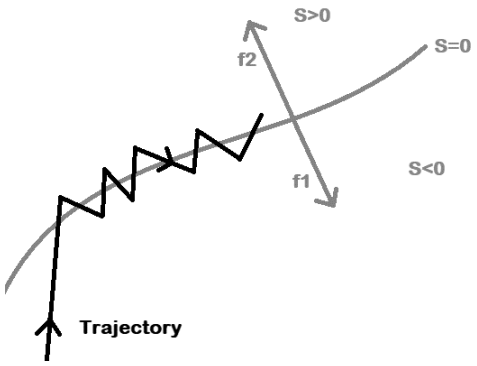

Fig. 5. Surface and Trajectory for Sliding Mode Control

V. SIMULATION RESULTS AND DISCUSSIONS

The varying input irradiance was realized using a repeating table block in Simulink to simulate step rise, step fall, ramp rise and ramp fall in irradiance. A saturation block limited the duty cycle between 0.05 and 0.95 and that helped in overcoming negative values and simulation errors.

The PV panel was connected directly to the boost converter, which was in turn connected to a 150 Ω resistive load. The MPPT block implemented the three proposed MPPT techniques and output the required pulses for the converter.

A. Perturb and Observe Algorithm

The P&O algorithm was realized completely using MATLAB codes. A constant step size of ΔD=0.2 % was used.

B. Fractional Short-Circuit Current Technique

A pulse of 5.0% duty cycle was generated every 0.073 s. The timing was chosen to prevent the signal from being sampled when there is a step change in irradiance and so that the signal is sampled fast enough to be able to track small changes in I_{sc}. The pulses closed a switch which short-circuited the terminals of the converter. During this time, I_{sc} was measured and its value stored. When the pulse signal drops to zero, the switch opened and power flowed to the load again. The latest value of I_{sc} was compared with the instantaneous current, I, and by subtracting them, an error signal was generated. D was decreased by ΔD= 2 % if the error >0, remained the same if error=0 or increased by ΔD= 2 % if error <0 after each iteration.

C. Sliding Mode Control

The inputs, current and voltage, were differentiated with respect to time. k=V/I + dV/dI was calculated and fed to a switching circuit that outputs either '1' or '-1' depending on set conditions on its input. Division by zero is overcome by replacing dI and I with an infinitesimal value if any of them is zero.

The output of the switching circuit is mapped in the range [-1, 1] to [0, 1] to give a signal Q. If the operating point is above S, Q is 1, else Q is 0. To overcome the situation where Q changes at an unrealizable frequency, and also, to be able to compare the three algorithms discussed in this paper, similar switching frequencies shall be used. The value of the control signal Q was held for 1.67×10^{-5} s in a Zero-Order Hold block. The output of this block is the signal E. The value of E could change only once in $2\times1.67\times10^{-5}$ s. This is equivalent to a maximum PWM frequency of 30 kHz. The frequency of E was therefore limited to 30 kHz. E was fed directly to the converter. In this system, there was no need for a PWM generator.

D. Discussions

Three MPPT algorithms were compared using performance indicators which include tracking time, level of oscillations at steady-state and their ability to track the MPP under step changes and ramp changes in irradiance. The tracking time was taken as the time taken to reach and stay at MPP from an initial Duty Cycle of 0.05 and at an irradiance of 1000 W/m^2. The tracking times have been measured using measurement cursors in Simulink. At MPP, the peak-to-peak amplitude of oscillation was also measured and tabulated in Table III. The irradiance followed the profile shown in Fig. 6. The power attained using the different MPPT algorithms are shown in Fig. 7.

It is observed (see Fig. 7) that the real MPP was not tracked using FSCC technique. The estimated maximum power reached using FSCC technique lie lower than the real maximum power reached using P&O and SMC. It is also confirmed from Fig. 11 that currents reached were lower than I_{mpp} using FSCC. Multiple spikes are observed in its power curve. The spikes correspond to the times when I_{sc} were being measured. During ramp changes in irradiance, again MPP was not tracked because the instantaneous current already changed. In consequence, I_{sc} also changed. Since only the last sampled I_{sc} was used to estimate I_{mpp}, this brought the system further away from the MPP. This is confirmed in Fig. 9 and Fig. 8 where large deviations from the required Duty Cycles and voltages are observed during ramp changes in irradiance. After I_{sc} had been sampled and then, the irradiance changed in a step, the MPP was not tracked until I_{sc} was sampled again. This can be seen in the power curve of Fig.7 at 0.3 s. More frequent sampling would definitely improve the tracking ability but that would also disrupt power flow and introduce harmonics which will in turn cause heating in the system leading to lower efficiency.

P&O performed better than FSCC and was able to track the MPP under all varying irradiance conditions. However, the system experienced sustained oscillations at steady state. The oscillations' amplitudes could be minimized by reducing the step size of the Duty Cycle; however, the tracking time would decrease.

The performance using SMC was the best amongst the three. A very small tracking time of 15.8 ms and steady-state amplitude of 0.014 V were achieved at 1000 W/m2. From Fig. 10, it is observed that D remained 0 for a longer time because the operating point was not on the surface S. Once on the surface, it is observed that D switched between 1 and 0 as the system slides on S. The maximum frequency of the signal D is 30 kHz. However, the rigorous switching of the duty cycle in a short period of time is the key factor to a good transient performance. This may have an effect on the life cycle of transistors/FETs used to do the switching.

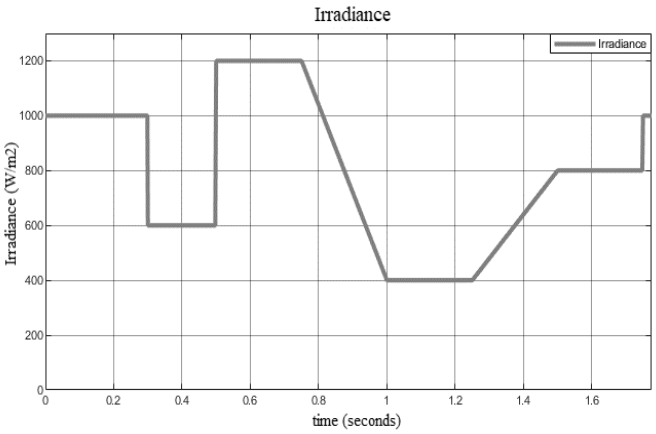

Fig. 6. Variation of the Irradiance

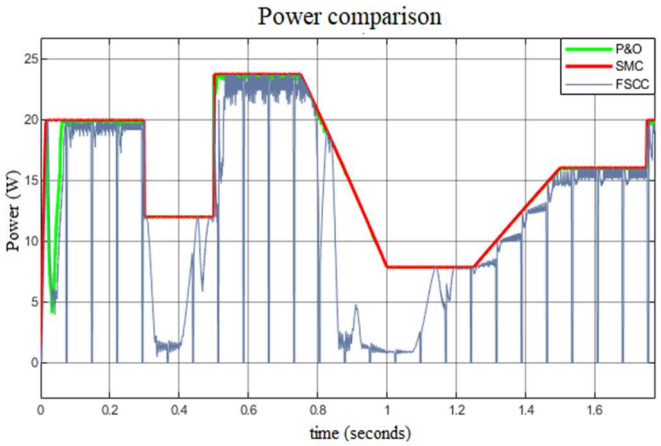

Fig. 7. Power comparison

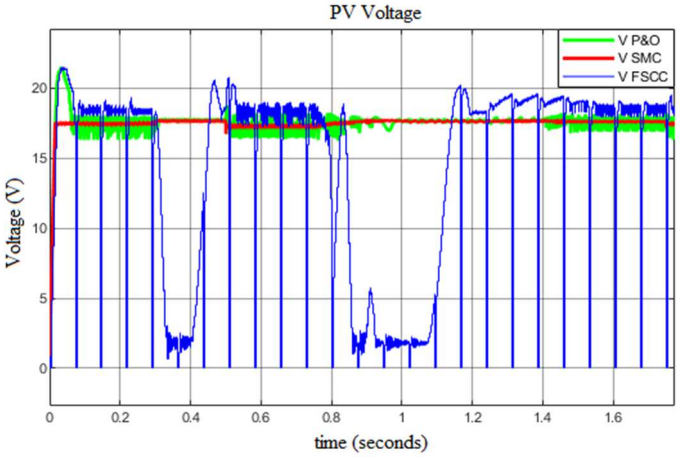

Fig. 8. Variation of the PV Voltage

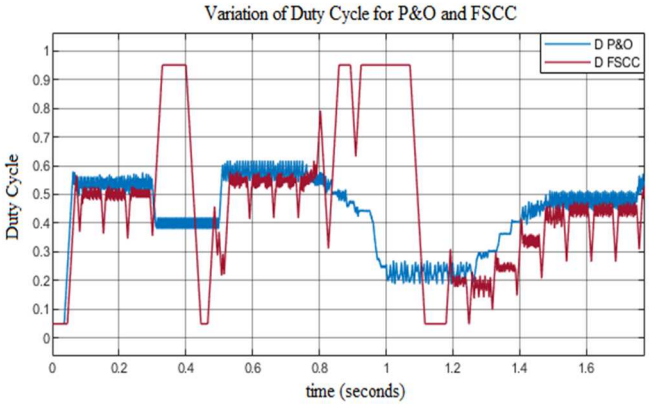

Fig. 9. Variation of the Duty Cycle for P&O and FSCC

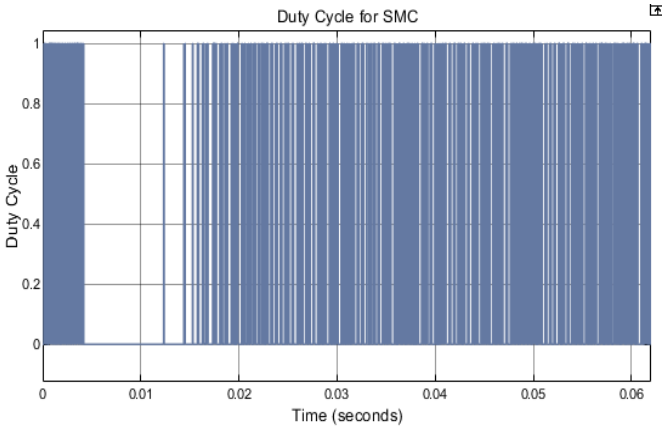

Fig. 10. Variation of the Duty Cycle for SMC

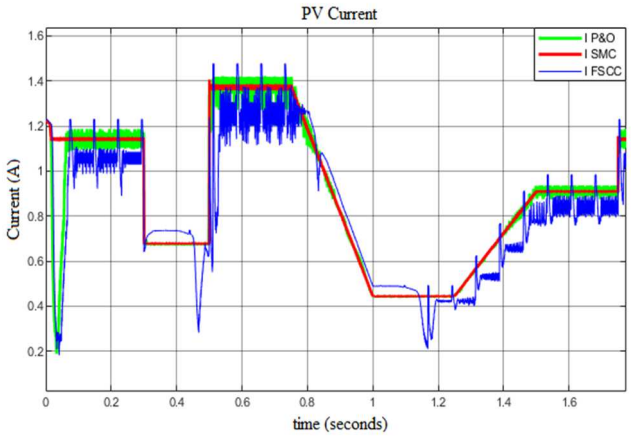

Fig. 11. Variation of PV Current

TABLE III. SIMULATION RESULTS

	P&O	**FSCC**	**SMC**
Tracking time (ms)	61.881	72.852	15.827
Pk-Pk amplitude at steady state (V)	0.5652	1.116	0.0142
Peak power reached at 1 kW/m2 (W)	19.95	19.68	19.95
Ability to track step increase in irradiance	✔	✔	✔
Ability to track Step decrease in irradiance	✔	✔	✔
Ability to track Ramp increase in irradiance	✔	✘	✔
Ability to track Ramp decrease in irradiance	✔	✘	✔

VI. CONCLUSION

A photovoltaic system consisting of a PV panel (single-diode model), a boost converter and a resistive load was modeled in MATLAB/Simulink environment. The boost converter acted as an interface between the PV Panel and the load. Three very dissimilar MPPT techniques namely, P&O, SMC and FSCC were investigated and their performance compared. The MPPT algorithm generated the control signal on the basis of PV panel's output current and voltage measurement to control the converter.

It was shown that P&O and SMC had accurate responses to changing irradiance as they were able to track the MPP and all three MPPT techniques were able to track the MPP at constant irradiance. SMC gave the best transient performance by achieving the lowest tracking time of 15.8 ms, followed by P&O and lastly FSCC.

REFERENCES

[1] Nadarajah Kannan and DivagarVakeesan, "Solar energy for future world:-A review. *Renewable and Sustainable Energy Reviews"*, pp. 1, 2014.

[2] Ankita Gaur and G. N. Tiwari. "Performance of Photovoltaic Modules of Different Solar Cells." *Journal of Solar Energy*, pp. 2, 2013.

[3] B.K. Nayak, A.Mohapatra and B.Misra. "Non Linear I-V Curve Of PV Module: Impacts On MPPT And Parameters." *International Journal of Engineering Research & Technology (IJERT)*, pp. 1, 2012.

[4] H.Ziar, S.Mansourpour, E.Afjei and M.kazemi. "Bypass diode characteristic effect on the behaviour of solar PV array at shadow condition." *2012 3rd Power Electronics and Drive Systems Technology (PEDSTC)*, pp. 3, 2012.

[5] S. Kolsi1, H. Samet and M. Ben Amar. "Design Analysis of DC-DC Converters Connected to a Photovoltaic Generator and Controlled by MPPT for Optimal Energy Transfer throughout a Clear Day." *Journal of Power and Energy Engineering*, pp. 1, 2014.

[6] Nicola Femia , Giovanni Petrone, Giovanni Spagnuolo and Massimo Vitelli. Power Electronics and Control Techniques for Maximum Energy Harvesting in Photovoltaic Systems. Taylor & Francis Group, LLC, 2013.

[7] Pooja Sahu, Deepak Verma and Dr. S Nema. "Physical Design and Modelling of Boost Converter." *2016 International Conference on Electrical Power and Energy Systems (ICEPES)* . Bhopal, India: Maulana Azad National Institute of Technology, pp. 2, 2016.

[8] Muhammad H. Rashid.. Power Electronics Handbook. Pensacola, Florida: ACADEMIC PRESS, 2001.